International Journal of Multidisciplinary Research and Growth Evaluation
ISSN: 2582-7138
Received: 07-09-2021; Accepted: 09-10-2021
www.allmultidisciplinaryjournal.com
Volume 2; Issue 6; November-December 2021; Page No. 32-37

Development of wind and solar based ac micro grid with power quality improvement for local nonlinear load using MLMS

Rahamath Uzma [1], Y Chintu Sagar [2]
[1-2] Dr K V Subbareddy College of Engineering for Women, Kurnool Dist., Andhra Pradesh, India
Corresponding Author: **Rahamath Uzma**

Abstract
This work proposes a microgrid (μ-grid) integrating wind and solar photovoltaic (PV) resources, along with the battery energy storage (BES) to the three-phase grid feeding the nonlinear load. The μ-grid disconcerted by probabilistic nonlinear time dependent parameters and their effects are compensated by cohe- sive controllers used for utility grid side voltage source converter (GVSC) and machine side voltage source converter (MVSC). The switching controls and the reconfigurability of the μ-grid are addressed on imperative aspects of improving power quality (PQ), power reliability, nonlinear load compensation, and economic utilization of resources. The nonlinear load compensation and PQ enhancement are achieved by executing modified version of the adaptive filtering technique including "momentum"-based least mean square (MLMS) control technique, utilized for providing the switching control signals to the GVSC. It utilizes two preceding gradient weights for obtaining updated weight thereby improving the convergence rate and overcoming the limitation of conventional control of the same family. The MVSC acquires its switching sig- nals from conventional vector control scheme and the encoderless estimation of speed and rotor position of the synchronous generator driven by wind turbine through back electromotive force control technique. The external environmental disturbances are overcome by utilizing perturb and observe (P&O) maximum power point (MPP) for wind optimal power extraction and adaptive P&O with variable perturbation step size for solar MPP estimation. Test results are obtained from the laboratory prototype under steady-state and dynamic conditions, including altering wind speed, intermittent solar insolation, and variable load conditions. The PQ issues are addressed and investigated successfully.

Keywords: AC microgrid, maximum power point (MPP) and power quality (PQ), momentum-based least mean square (MLMS), solar photovoltaic (PV) power generation, maximum power point (MPP)

1. Introduction
THE EXPANSION of economies has led to the rise of en- ergy demand. By 2050, the demand may double or even triple as an outcome of population rise [1]. The conservation of energy, research on renewable energy resources (RERs) appli- cability and halting the dependency on fossil fuels, is of utmost importance. The RERs are dominated by their intermittency and geographic location availability. The variability of the energy supply is overcome by the use of storage systems, like battery energy storage (BES) [2-3]. As an effective application, micro- grid (μ-grid) acts as a localized entity, which is low or medium voltage, including sources of electricity, BES, and loads that op- erate either in grid-connected or off-grid mode. μ-grid provides promising alternatives of electricity generation. The aim of the power providers is to feed the highest level of generated power into the grid when the electricity price and the load demand are at its highest value. This results in recovering the additional rev- enue utilized in the installation. The combination of solar energy conversion system (SECS) and wind energy generation system (WEGS) increases the system efficiency and power reliability [4-5]. Their combination provides energy surety and continu- ity as both the resources complement each other and cut down the reserve or storage requirements. In this work, the hybrid sys- tem consists of single stage SECS and synchronous generator (SG) driven by wind turbine producing wind energy.
To control and regulate the voltage and frequency of the gen- erated electricity from WEGS to fulfill the grid code compliance [6], full rated voltage source converters (VSCs) are adapted as an interface between the machine and the utility grid [7]. Two back-to-back connected VSCs, i.e., ac/dc converter, named as machine side VSC (MVSC), a dc link, and a dc/ac inverter named as grid side VSC (GVSC) are implemented for variable revolutions per minute (RPM) operation of the system. The MVSC regulates the SG output power with variable RPM into dc power. It ad- justs the current and torque of the SG.

The GVSC upholds the dc link voltage and synchronizes the ac generated power by the wind turbine driven SG with the power of the utility grid. Grid-connected installations provide the possibility of continu- ous power flow at the instances where the generation from solar and wind, is not enough to fulfill requirement and absorbs the ex- cessive power when the generation is more than demand. As an outcome, storage requirements are decreased [8]. Vergara *et al.* have investigated the optimal operation of the μ-grid for the grid connected and the isolated mode with distributed generator unit, BES and wind turbines. Singh *et al.* [10] have analyzed the seamless transition of the μ-grid. The renewable-based μ-grid synchronization to the grid is considered. Xiao *et al.* [11] have studied the frequency instability issues arising from the dispersed wind power associated to the weak grid. An analy- sis is carried out by considering different transition operational modes. For upholding the stable dc-link voltage, the fluctuating output from the renewable energy sources, needs to be smoothed out [12-13]. Lumbreras *et al.* [14] have analyzed a modified power topology where the boost inductor and the filter capaci- tance, are substituted by the phase inductance of the generator of WEGS. This reduces the system losses, cost, and size. When the generation from renewables is being considered, then the storage systems find their way for providing the continuous power. The integration of the appropriate energy storage being implemented in the μ-grid for the fault tolerance reconfigurability is being investigated in [15-17]. Nguyen *et al.* [17] have described the wind optimal power dispatch strategy by reducing the BES capacity. The capacity is determined based on first-order low-pass filter (FLF) where the optimized time constant is used in sampling time.

Grid integration to renewable energy sources provides the al- ternative for continuous power supply. An increased penetration of renewables to the power grid under normal and abnormal op- erating conditions is aimed to provide the desired power support. Hadjidemetriou *et al.* [18] and Chen *et al.* [19] have examined the grid code compliance by introspecting the renewable energy source penetration into the grid. The wind generation system integration to the utility grid, poses the importance of consider- ation of the issues of power quality (PQ), voltage fluctuations at the point of common interconnection (PCI), voltage unbalance, sudden voltage variations, such as voltage sag and swell. Muljadi *et al.* [20] have illustrated the technical challenges imposed by the renewables. The operating characteristics of the components are studied to relate with the issues deteriorating PQ.

In this paper, the solar photovoltaic (PV) array (single stage) is linked to a BES at the dc link through the bidirectional dc–dc converter. It manages the charging and discharging of the BES. It also eliminates the second-order harmonic that appears in the battery current enhancing battery vitality in comparison to the configuration, where the BES is connected directly to the dc link and in which, during dynamic conditions, the fluctuations in the dc link, are reflected directly on the battery current and harm the battery life.

In the proposed work, MVSC is gated by the switching pulses obtained from the effective use of the vector control (VC). The VC permits the speed control under diverse range. From the per- formance view point, the machine is adapted as corresponding dc machine (separately excited). The same control, when im- plemented for ac machine, is extended by making an allowance for machine rotating in synchronously rotating reference frame (*d*–*q*). In the steady-state condition, the sinusoidal quantities are reformed as dc quantities [21]. The SG rotor position and speed are assessed by using encoderless back electromotive force (BEMF) scheme and utilized by VC [22]. However, nu- merous rotor speed and position estimation techniques have been proposed in the literature, which vary in their application de- pending on the objective [23-25].

2. Control Methodology

The control algorithms for proposed system consist of three subsections. First is the momentum-based LMS (MLMS)-based switching control for GVSC, second is the VC-based switch- ing control for the MVSC, and third is for the bidirectional converter control. These control algorithms, together with the MPP techniques for wind and solar, introspect the effective- ness of the system performance under steady-state and dynamic conditions.

3. Control Methodology

The control algorithms for proposed system consist of three subsections. First is the momentum-based LMS (MLMS)-based switching control for GVSC, second is the VC-based switch- ing control for the MVSC, and third is for the bidirectional converter control. These control algorithms, together with the MPP techniques for wind and solar, introspect the effective- ness of the system performance under steady-state and dynamic conditions.

A. MPP Extraction Scheme

The solar insolation level and wind speed are inconsistent in nature and they vary with time and location. However, the system utilizing these two renewables imposes the individual implementation of the optimal power extraction technique. The P&O control scheme effectively tracks the wind MPP and the solar MPP is estimated using adaptive P&O with variable per- turbation step size.

1. Wind-P&O Control Scheme: Fig. 2 shows the flowchart of the wind MPP scheme. P&O scheme [35] is the most pop- ular and simplistic control approach, which identifies the MPP from the nonlinear characteristics of wind. This algorithm ad- justs the wind turbine driven generator's speed ($\omega_{\text{gen est}}$) in order to achieve the MPP (P_{wind}). The SG speed is perturbed in the given direction, while observing the power drawn from the SG. If the power drawn from the SG increases, this indicates that the optimal point of operation has traversed toward the MPP and as a result, the SG speed must be perturbed in the same direction. On the contrary, if the power drawn from SG decreases, the op- timal point of operation has navigated away from the MPP and therefore, the perturbing SG speed must be reversed henceforth. The governing equations are given as

ωgen ref (n)= ωgen ref ($n-1$)+ $\Delta\omega$gen;

$\Delta P_{\text{gen}} > 0$ and $\Delta\omega_{\text{gen est}} > 0$

6) The feed-forward terms of wind and solar enhance the system dynamic response if

$\Delta P_{\text{gen}} < 0$ and $\Delta\,\omega_{\text{gen est}} < 0$ (1)

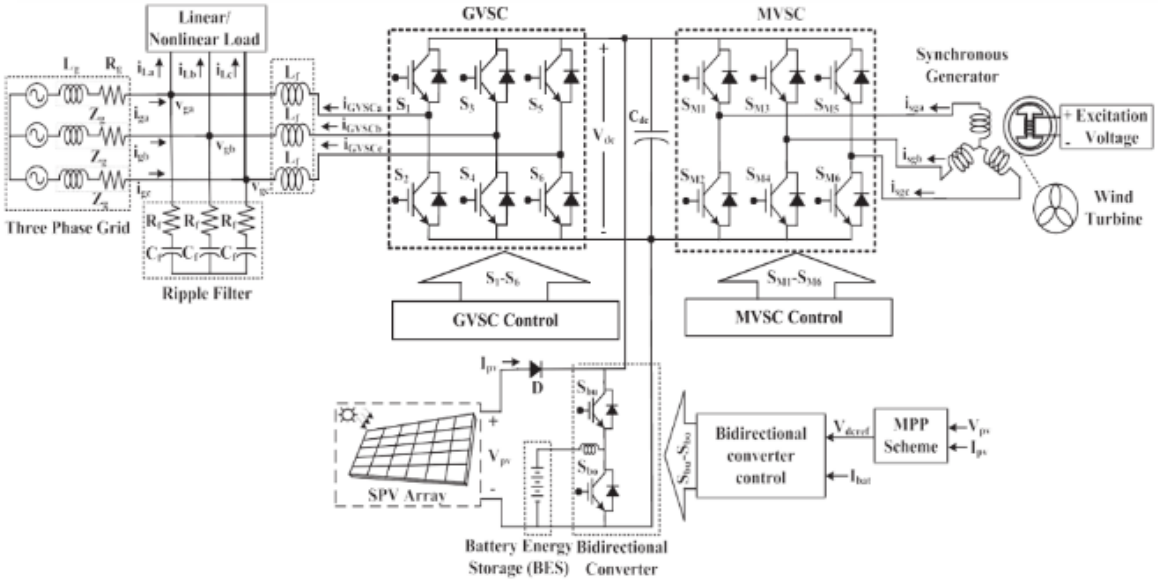

Fig 1: System configuration.

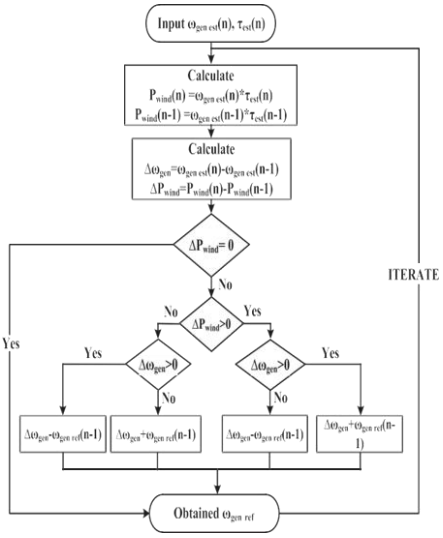

Fig 2: Flowchart of the wind-P&O MPP scheme.

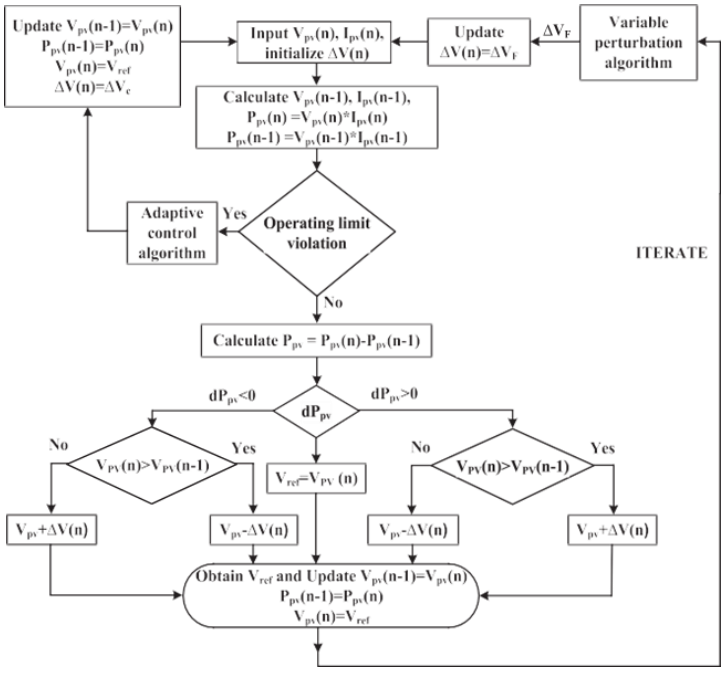

Fig 3: Flowchart of the solar-adaptive P&O MPP technique.

2. Solar-Adaptive P&O MPP Control: Fig. 3 shows the flowchart for the solar MPP scheme. The adaptive P&O MPP control overcomes the oscillations issues of fixed step-based MPP techniques by introducing a variable perturbation step size. The control estimates the MPP operating point by using a prod- uct of short-circuit current and optimal proportionality constant [36]. The tuning procedure of the perturbation step size is based irradiation level.

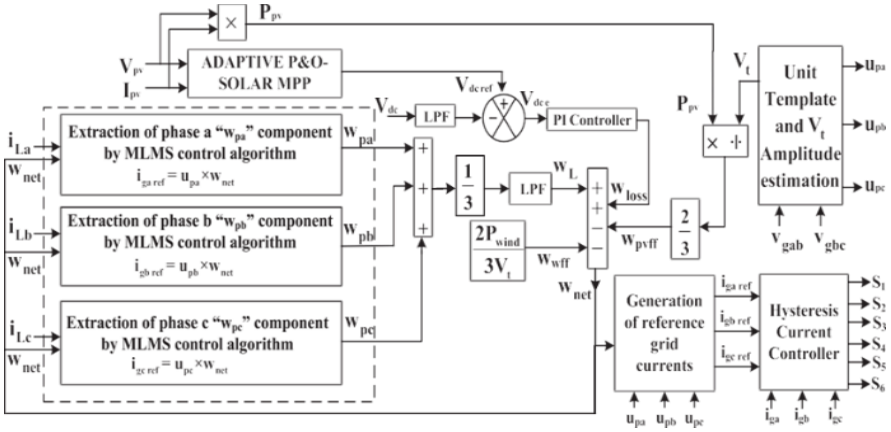

Fig 4: Control structure for GVSC.

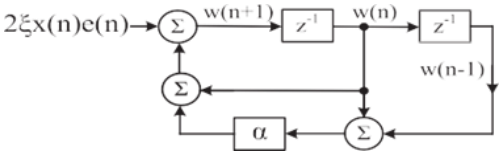

Fig 5: MLMS algorithm.

B. GVSC Switching Control

Fig. 4 shows the control scheme for the GVSC. For the time in- variant system with stochastic inputs like variable wind and solar conditions, the PQ enhancement and compensation of the load current distortion is carried out by using adaptive control-based MLMS control. It provides the switching pulses to the GVSC. The control is an advancement in the family of the least square algorithm. Varying system conditions and uncertainty in param- eters are handled easily by MLMS. The "momentum" factor is added to provide faster convergence rate. It uses the preceding gradient and updates the weight without affecting system com- plexity. It accelerates the convergence process and effectively compensates the load harmonics with noise polluted input sig- nals.

4. Results and Discussion

The experimental validation of wind solar-based ac microgrid system is carried on the developed hardware prototype. The wind turbine is emulated by the dc motor (BENLEC Make) coupled to the SG (BENLEC Make). The variable wind speed operation is realized by using back-to-back associated VSCs (SEMIKRON Make). The solar PV array characteristics are simulated through solar PV simulator (Tera Sas Make). Nonlinear load currents, SG, and grid currents are sensed by means of Hall-Effect cur- rent sensors (LA55P). Grid voltage V_{dc}, and V_t are sensed by Hall-Effect-based voltage sensors (LV25-P). These sensed sig- nals are processed according to the control algorithm by digital signal processor (DSP)-based dSPACE-1202 Micro Lab Box. The optocouplers (6N136) provide the switching pulses to the VSCs. They provide the isolation between the VSC gate driver circuit and the DSPACE. The digital signal oscilloscope (DSO) and PQ analyzer are used to record the test results of the system. The component specifications and detailed system parameters are mentioned in Appendix.

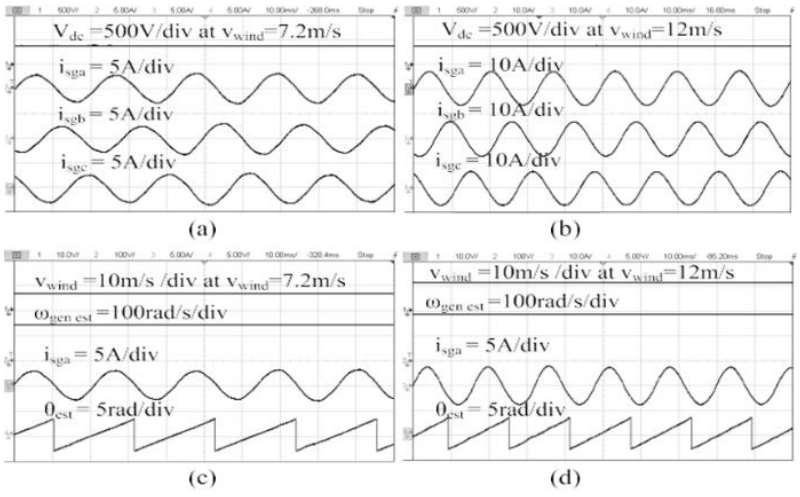

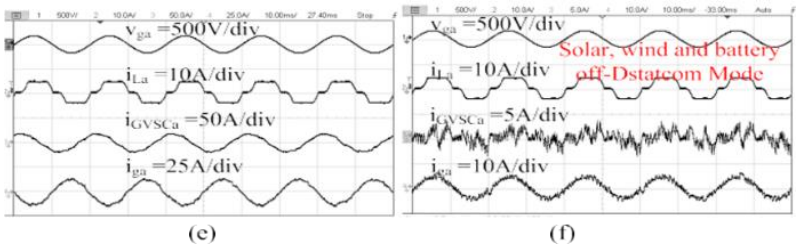

Fig 8: Response of the microgrid at steady-state condition.

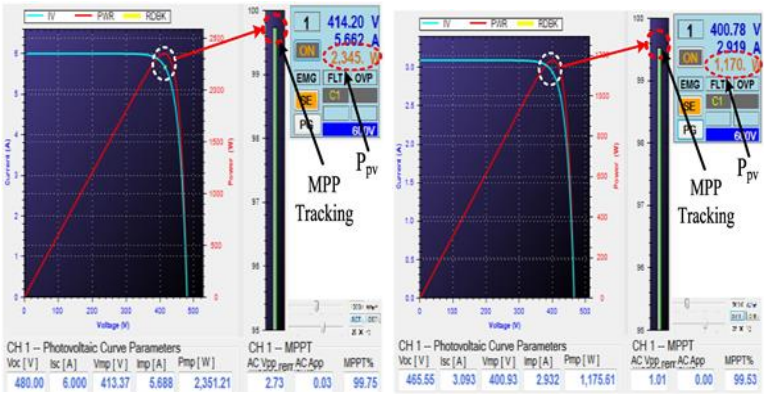

a. b.

Fig 9: Solar MPP tracking performance at (a) full solar insolation; (b) half solar insolation.

Is OFF, then the system operates under DSTATCOM mode. The GVSC supplies the compensating currents. The grid currents are sinusoidal and undergoes phase reversal and are shown in Fig. 8(f).The solar MPP performance is shown in Fig. 9. At maximum solar insolation, the MPP achieved is 99.75% provid- ing 2.34 kW, whereas at half solar insolation, the MPP tracked is 99.53% providing 1.17 kW solar power. Fig. 10 shows the nonlinear load parameters along with the current THD 17.9% and voltage THD equal to 1.95%, depicting the presence of harmonics.

A. Response of Microgrid under Wind Speed Change

The wind speeds are inconsistent and their effects have to be analyzed for proper functioning of the microgrid. Fig. 11(a) and (b) show the dc-link voltage and the ac grid terminal voltage along with the grid voltage of one phase under wind speed rise and fall. The transient in the dc-link voltage is overcome by the bidirectional converter control and the dc-link voltage is maintained to its perpetual value by the bidirectional converter.

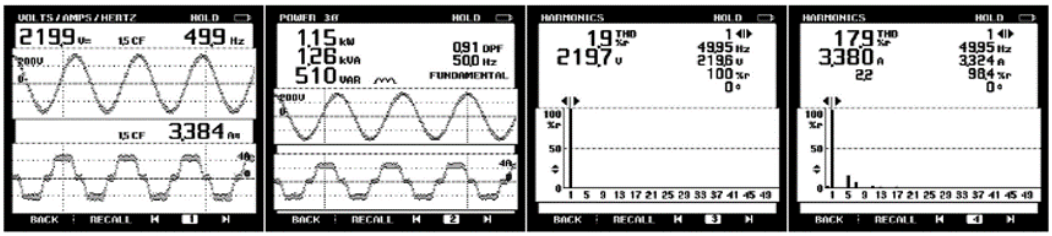

Fig 10: Load profile parameters.

5. Conclusion

The proposed wind-solar ac microgrid has been designed and implemented to illustrate its improved PQ performance for local nonlinear load using MLMS adaptive control. The weight com- ponent and system performance using MLMS has been found with reduced oscillations. Effectiveness of the MLMS is real- ized through successful harmonic elimination, extraction of load current fundamental component with low static error, and faster convergence rate. The wide range of wind speeds, solar inso- lation, and load variations have been considered and the test results obtained from the prototype provide exceedingly well performance for the entire operational range.

The grid current THD has been found well within the IEEE 519 harmonic Standard. The proposed system has operated well under all the dynamic conditions as well as the PQ issues are mitigated satisfactorily.

Appendix

A. *SG parameters:* 415 V, 5 hp, R_s = 3.1 Ω, poles = 4, field excitation voltage: 220 V.
B. *DC motor:* 220 V, 19 A, 5 hp.
C. *Wind speed range:* 7–12 m/s.
D. *DC-link voltage:* V_{dc} : 400 V.
E. *Solar PV array:* 2.4 kW.
F. *Parameters of BES:* 240 V, 56 Ah.
G. *Ripple flter parameters:* R_f = 5 Ω, C_f = 10 μF.
H. *PI controller gains:* k_{iloss} = 0.4; k_{ploss} = 0.75; k_{igen} = 0.2; k_{pgen} = 0.03.

A. Controller parameters: $\xi = 0.0087$; $\alpha = 0.7$.
B. Grid parameters: $v_{gab} = 220$ V, 50 Hz.

References

1. R. Cuzner, "The socially responsible microgrid," *IEEE Electrific. Mag.*, vol. 6, no. 4, pp. 2–5, Dec. 2018.
2. P. J. Chauhan, B. D. Reddy, S. Bhandari, and S. K. Panda, "Battery energy storage for seamless transitions of wind generator in standalone micro- grid," *IEEE Trans. Ind. Appl.*, vol. 55, no. 1, pp. 69–77, Jan./Feb. 2019.
3. M. Farhadi and O. Mohammed, "Energy storage technologies for high- power applications," *IEEE Trans. Ind. Appl.*, vol. 52, no. 3, pp. 1953–1961, May/Jun. 2016.
4. X. Hou *et al.*, "Distributed hierarchical control of AC microgrid operat- ing in grid-connected, islanded and their transition modes," *IEEE Access*, vol. 6, pp. 77388–77401, 2018.
5. S. Boudoudouh and M. Maaroufi, "Renewable energy sources integration and control in railway microgrid," *IEEE Trans. Ind. Appl.*, vol. 55, no. 2, pp. 2045–2052, Mar./Apr. 2019.
6. R. Millner, C. Smith, R. Jaddivada, and M. Ilic, "Component standards for stable microgrids," *IEEE Trans. Power Syst.*, vol. 34, no. 2, pp. 852– 863, Mar. 2019.
7. Radwan and Y. Mohamed, "Grid-connected wind-solar cogenera- tion using back-to-back voltage source converters," *IEEE Trans. Sustain. Energy*, to be published.
8. M. Al-Masri and M. Ehsani, "Feasibility investigation of a hybrid on- grid wind photovoltaic retrofitting system," *IEEE Trans. Ind. Appl.*, vol. 52, no. 3, pp. 1979–1988, May/Jun. 2016.
9. P. P. Vergara *et al.*, "A generalized model for the optimal operation of mi- crogrids in grid-connected and islanded droop-based mode," *IEEE Trans. Smart Grid*, to be published.
10. Singh, G. Pathak, and B. K. Panigrahi, "Seamless transfer of renewable- based microgrid between utility grid and diesel generator," *IEEE Trans. Power Electron.*, vol. 33, no. 10, pp. 8427–8437, Oct. 2018.
11. Z. Xiao, M. Zhu, Y. Huang, J. M. Guerrero, and J. C. Vasquez, "Coordi- nated primary and secondary frequency support between microgrid and weak grid," *IEEE Trans. Sustain. Energy*, to be published.
12. P. Malysz, S. Sirouspour, and A. Emadi, "An optimal energy storage con- trol strategy for grid-connected microgrids," *IEEE Trans. Smart Grid*, vol. 5, no. 4, pp. 1785–1796, Jul. 2014.
13. Y. Shan, J. Hu, K. W. Chan, Q. Fu, and J. M. Guerrero, "Model pre- dictive control of bidirectional dc-dc converters and ac/dc interlinking converters—a new control method for PV-wind-battery microgrids," *IEEE Trans. Sustain. Energy*, to be published.
14. Lumbreras *et al.*, "Analysis and control of the inductor less boost recti- fier for small-power wind-energy converters," *IEEE Trans. Ind. Appl.*, vol. 55, no. 1, pp. 689–700, Jan./Feb. 2019.
15. S. S. Thale, R. G. Wandhare, and V. Agarwal, "A novel reconfigurable microgrid architecture with renewable energy sources and storage," *IEEE Trans. Ind. Appl.*, vol. 51, no. 2, pp. 1805–1816, Mar./Apr. 2015.
16. S. A. Saleh, R. Meng, and R. McSheffery, "Evaluating the performance of digital modular protection for grid-connected permanent-magnet- generator-based wind energy conversion systems with battery storage sys- tems," *IEEE Trans. Ind. Appl.*, vol. 53, no. 5, pp. 4186–4200, Sep./Oct. 2017.
17. Nguyen and H. Lee, "Power management approach to minimize battery capacity in wind energy conversion systems," *IEEE Trans. Ind. Appl.*, vol. 53, no. 5, pp. 4843–4854, Sep./Oct. 2017.
18. L. Hadjidemetriou, E. Kyriakides, and F. Blaabjerg, "A new hybrid PLL for interconnecting renewable energy systems to the grid," *IEEE Trans. Ind. Appl.*, vol. 49, no. 6, pp. 2709–2719, Nov./Dec. 2013.
19. X. Chen *et al.*, "Integrating wind farm to the grid using hybrid multi ter- minal HVDC technology," *IEEE Trans. Ind. Appl.*, vol. 47, no. 2, pp. 965–972, Mar./Apr. 2011.
20. Muljadi and H. E. McKenna, "Power quality issues in a hybrid power system," *IEEE Trans. Ind. Appl.*, vol. 38, no. 3, pp. 803–809, May/Jun. 2002.
21. D.-W. Chung and S.-K. Sul, "Analysis and compensation of current mea- surement error in vector-controlled AC motor drives," *IEEE Trans. Ind. Appl.*, vol. 34, no. 2, pp. 340–345, Mar./Apr. 1998.
22. P. Kshirsagar and R. Krishnan, "High-efficiency current excitation strat- egy for variable-speed nonsinusoidal back-EMF PMSM machines," *IEEE Trans. Ind. Appl.*, vol. 48, no. 6, pp. 1875–1889, Nov./Dec. 2012.
23. L. Sheng, W. Li, Y. Wang, M. Fan, and X. Yang, "Sensorless control of a shearer short-range cutting interior permanent magnet synchronous motor based on a new sliding mode observer," *IEEE Access*, vol. 5, pp. 18439– 18450, 2017